r_{shell} = reaction rate in shell, moles/min. equivalent of catalyst sulfonic acid groups in shell
t = time, min.

Greek Letters

α = fraction of water produced in swelling period which remains in particle
γ = fraction of catalytic sites located on particle peripheries
ρ_W = moles of water per unit volume in shell, moles/cu. cm.
$\theta = \dfrac{3\alpha N_c(1-\gamma)r_{shell}t}{4\pi r_{p0}^3 \rho_W N_p}$, dimensionless

Subscripts

A = alcohol
W = water
0 = value at $t = 0$
s = value at $r_c = 0$

LITERATURE CITED

1. Polyanskii, N. G., *Russ. Chem. Rev.*, 39, 244 (1970).
2. Satterfield, C. N., "Mass Transfer in Heterogeneous Catalysis," M.I.T. Press, Cambridge (1970).
3. Gupta, V. P., and W. J. M. Douglas, *AIChE J.*, 13, 883 (1967).
4. Gruber, P. E., and H. Noller, *Z. Phys. Chem.* (Frankfurt), 41, 353 (1964).
5. Helfferich, "Ion Exchange," McGraw-Hill, New York (1962).
6. Bortnick, N. M., U.S. Pat. 3,037, 052 (1962).
7. Frilette, V. J., E. B. Mower, and M. K. Rubin, *J. Catalysis*, 3, 25 (1964).
8. Heath, H. W., Jr., MChE thesis, Univ. Delaware, Newark (1971).
9. Kunin, R., E. Meitzner, and N. Bortnick, *J. Am. Chem. Soc.*, 84, 305 (1962).
10. Venuto, P. B., L. A. Hamilton, P. S. Landis, and J. J. Wise, *J. Catalysis*, 5, 81 (1966).
11. Gates, B. C., J. S. Wisnouskas, and H. W. Heath, Jr., *ibid.*, in press.
12. Zundel, G., "Hydration and Intermolecular Interaction," Academic Press, New York (1969).
13. Goldring, L. S., in "Ion Exchange," Vol. 1, J. A. Marinsky, ed., pp. 205-225, Marcel Dekker, New York (1966).
14. Reichenberg, D., and W. F. Wall, *J. Chem. Soc.* (London), 1956, 3364 (1956).

Manuscript received June 15, 1971; revision received September 3, 1971; paper accepted September 7, 1971.

Dynamics of Diffusion and Adsorption in a Single Catalyst Pellet

MOTOYUKI SUZUKI and J. M. SMITH

Department of Chemical Engineering
University of California, Davis, California 95616

Exposing one face of a catalyst pellet to a pulse of tracer gas and analyzing the response at the opposite end provides a dynamic method for measuring the effective diffusivity of porous catalysts. The first and second moments of the response peak are shown to be a function of only D_e and the geometry of the pellet and detector chamber for a nonadsorbing, tracer-carrier system. Data obtained for alumina pellets of different densities illustrate the method.

For an adsorbing tracer, the first moment is a function of both D_e and the adsorption equilibrium constant. Measurements for an unconsolidated assembly of nickel/Kieselguhr particles, using the D_2-H_2 system, show that first-moment data are sufficient to calculate reasonably accurate values of the equilibrium adsorption. However, it appears to be difficult to obtain adsorption rate constants by this method.

Chromatographic measurements for beds of catalyst particles have been used [for example, (5, 8, 9)] to measure adsorption and intraparticle rate coefficients. This method relates the moments of the concentration peak at the exit of the bed to the various rate coefficients. Hence, the influence of all the transport effects, including axial dispersion, are measured. For studying only intraparticle effects it would be advantageous to eliminate the influence of axial dispersion. Chromatographic experiments with single pellets would accomplish this objective. In this paper a method is presented, and tested experimentally, for using single pellet chromatography to evaluate effective diffusivities and adsorption equilibrium data for porous catalysts. Isothermal operation and a first-order adsorption process are necessary. These restrictions are the same as required for bed chromatography. Isothermal conditions are approached by employing low concentrations of adsorbable component and pseudo first-order adsorption is achieved by the isotope technique (5, 9).

THEORY OF SINGLE-PELLET CHROMATOGRAPHY

Balder and Peterson (1) have developed the theory and experimental procedure for single pellet reactors operating

M. Suzuki is on leave from Institute of Industrial Science, University of Tokyo. Correspondence concerning this paper should be addressed to J. M. Smith.

at steady-state, and Gibilaro et al. (2) have proposed a transient procedure for investigating pore structure in single catalyst pellets. In the development that follows, a cylindrical pellet of length L with transport only in the axial direction is used (Figure 1). One circular face of the pellet adjoins a small, closed chamber which serves as a cell for a thermal conductivity detector. The other face is exposed to a continuous flow of gases. The time required for achieving uniform concentration in the detector chamber is approximately given by $(V_d/S)^2/D_{AB}$, while the corresponding relaxation time for the pellet is $L^2\,(\beta + \rho_B K_a)/D_e$. By making V_d/S small enough, the former time is negligible with respect to the latter and the concentration C_L in the detector chamber may be considered to be uniform. Then only the capacity effect of the detector volume need be considered in the equations that follow.

The concentration of diffusing component in the pellet shown in Figure 1 is described by the expression

$$D_e \frac{\partial^2 C}{\partial x^2} = \beta \frac{\partial C}{\partial t} + \rho_B \frac{\partial n}{\partial t} \tag{1}$$

where D_e is the effective diffusivity, β the total porosity, and the last term represents the rate of adsorption on the catalyst surface.

Suppose that the concentration at $x = 0$ is subjected to an impulse function

$$C = M\,\delta(t) \tag{2}$$

Then, assuming complete mixing in the detector volume, the boundary condition at $x = L$ is

$$D_e \left(\frac{\partial C}{\partial x}\right)_L = -\frac{V_d}{S}\frac{\partial C_L}{\partial t} \tag{3}$$

and initially

$$C = 0 \qquad x \geq 0 \tag{4}$$

For a first-order adsorption rate

$$\frac{\partial n}{\partial t} = k_a\left(C - \frac{n}{K_a}\right) \tag{5}$$

where n is the concentration of adsorbate on the surface, and k_a and K_a are the rate and equilibrium constants for adsorption.

Equations (1) and (5) with (4) can be written in the Laplace domain, designating transformed variables as $\overline{C}$ and $\overline{n}$, and then $\overline{n}$ eliminated, to yield

$$\frac{\partial^2 \overline{C}}{\partial X^2} = \Lambda^2 \overline{C} \tag{6}$$

Transforming Equations (2) and (3) gives

$$\overline{C} = M \quad \text{at} \quad X = 0 \tag{7}$$

$$\frac{\partial \overline{C}}{\partial X} = -\frac{\gamma L}{D_e} p\,\overline{C}_L \quad \text{at} \quad X = 1 \tag{8}$$

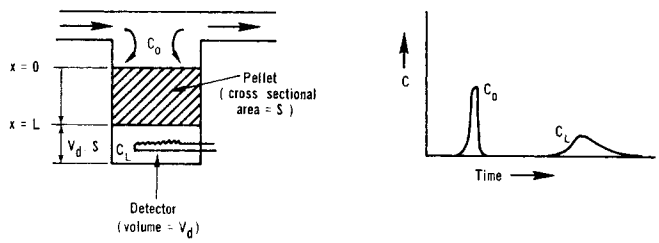

Fig. 1. Single-pellet chromatography.

where

$$\gamma = \frac{V_d}{S} \tag{9}$$

$$X = \frac{x}{L} \tag{10}$$

$$\Lambda = \{[\beta p + \rho_B\, k(p)]/D_e\}^{1/2}\, L \tag{11}$$

$$\frac{1}{k(p)} = \frac{1}{k_a} + \frac{1}{p\,K_a} \tag{12}$$

The solution of Equation (6), with (7) and (8), gives

$$\overline{C}(X) = M\left\{\cosh(\Lambda X) - \sinh(\Lambda X)\,\frac{\sinh\Lambda + \dfrac{\gamma L p}{D_e \Lambda}\cosh\Lambda}{\cosh\Lambda + \dfrac{\gamma L p}{D_e\Lambda}\sinh\Lambda}\right\} \tag{13}$$

Then the transform of the concentration in the detector volume $X = 1$ is

$$\overline{C}(1) = \overline{C}_L = \frac{M}{\cosh\Lambda + \dfrac{\gamma L p}{D_e\Lambda}\sinh\Lambda} \tag{14}$$

It is not necessary to invert $\overline{C}$ in order to compare theory with experiment. This is because the measurable moments m_n can be related to $\overline{C}_L$ by the expression

$$m_n = (-1)^n \lim_{p\to 0} \frac{d^n}{dp^n}(\overline{C}_L) \tag{15}$$

The nth moment function is defined in terms of the chromatographic peak at $x = L$ as

$$m_n = \int_0^\infty t^n\, C_L(t)\, dt \tag{16}$$

Using Equation (14) in (15), the first absolute moment μ_1 and second central moment μ_2' are given by

$$\mu_1 = \frac{m_1}{m_0} = \frac{L^2}{D_e}\left(\frac{\beta + \rho_B K_a}{2} + \frac{\gamma}{L}\right) \tag{17}$$

$$\mu_2' = \frac{\int_0^\infty (t-\mu_1)^2\, C_L(t)\, dt}{m_0} = \frac{m_2}{m_0} - \left(\frac{m_1}{m_0}\right)^2$$

$$= \left(\frac{L^2}{D_e}\right)^2\left[\frac{2}{3}\left(\frac{\beta + \rho_B K_a}{2} + \frac{\gamma}{L}\right)^2 + \frac{1}{3}\left(\frac{\gamma}{L}\right)^2\right] + \frac{L^2}{D_e}\frac{\rho_B K_a^2}{k_a} \tag{18}$$

For diffusion of an inert (nonadsorbable) component through the pellet $K_a = 0$ and Equations (17) and (18) become

$$\mu_1 = \frac{L^2}{D_e}\left(\frac{\beta}{2} + \frac{\gamma}{L}\right) \tag{19}$$

$$\mu_2' = \left(\frac{L^2}{D_e}\right)^2\left[\frac{2}{3}\left(\frac{\beta}{2} + \frac{\gamma}{L}\right)^2 + \frac{1}{3}\left(\frac{\gamma}{L}\right)^2\right] \tag{20}$$

Equations (17) to (20) relate the moments of the measured response at the detector to the effective diffusivity,

adsorption rate and equilibrium constants, porosity and length of the catalyst pellet, and to the geometry of the detector. For an inert system, first-moment data can be used with Equation (19) to determine the effective diffusivity when β, L, and γ are known. Alternately, first moments for pellets of different lengths can be used to evaluate D_e and β, if the latter is not known. Subsequently, first moments obtained for an adsorbing gas, using the same pellet, can be used with Equation (17) to obtain the equilibrium adsorption constant K_a. In principle, second-moment information and Equation (18) would give the adsorption rate constant k_a. However, experimental problems restrict this last possibility. The theory is tested in the following sections, first to evaluate D_e from data on inert systems with alumina pellets, and second to obtain D_e and K_a for H_2 in a Ni/Kieselguhr catalyst.

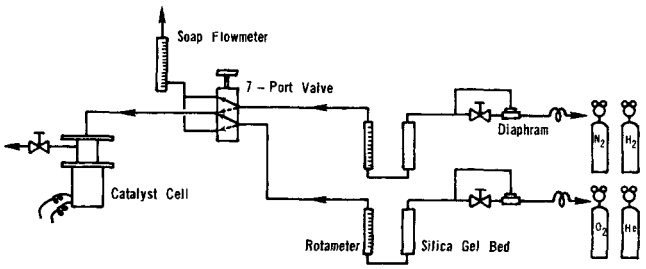

Fig. 2a. Schematic diagram of apparatus.

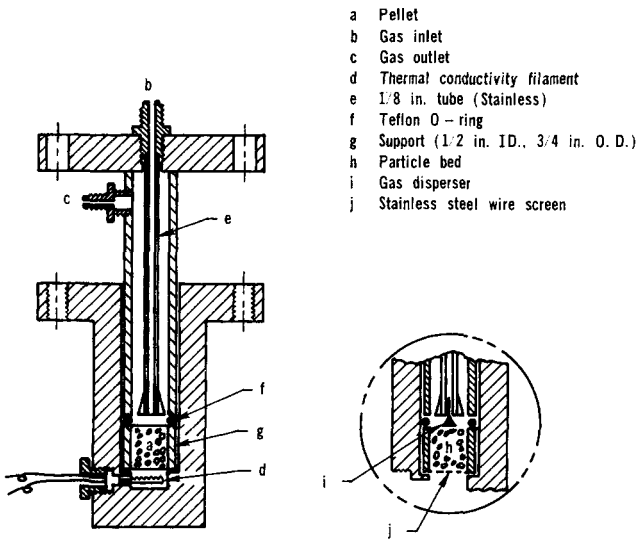

Fig. 2b. Details of catalyst holder.

DIFFUSION IN ALUMINA PELLETS

Apparatus and Procedure

Figure 2a is a flow diagram of the apparatus and Figure 2b shows the details of the cell holding the catalyst. The holder was made from an aluminum block. It is similar to that used by Balder and Peterson (*1*) except that the thermal conductivity filament (tungsten-rhenium) was located in the detector chamber (V_d = 0.70 cu.cm.) adjoining the face of the catalyst. Pellets were made by compressing Boehmite powder (average particle size about 70 microns) in a ring mold (I.D. = 1.33 cm.) with a mirror finish on the inside surface. The ring containing the pellet was tightly held in the catalyst holder by a Teflon O-ring (Figure 2b).

The gas was fed directly onto the upper end face of the pellet to ensure no film resistance at the gas-solid interface. The dead volume between the injection valve and the catalyst surface was reduced to about 1.0 cu.cm. The residence time in this volume was accounted for in calculating first moments.

The pure diffusing component was introduced into the carrier gas by operating the 7-port injection valve. The injection time was chosen so that the detector readings were as small as possible, consistent with an accurate chart reading on the detector. The maximum concentration of the peak was usually about 2% of the concentration in the injection sample, and was always less than 5%. The conductivity of the filament was detected with a constant-current bridge and recorded.

All data were obtained at 24°C. and 1 atm. total pressure.

Properties of Pellets

The properties of the four pellets, each of different density, are shown in Table 1. Total porosity β was measured using a

Table 1. Data for Alumina Pellets

Pellet no.	ρ_B, g./cu.cm.	Pelleting pressure, 10^3 lb.	L, cm.	β,°	β_a,°°	β_i,†	$\overline{r_a} \times 10^{-4}$, Å avg. macropore radius	System tracer	carrier	$\Delta\mu_1$ min.	D_e sq.cm./sec.	D_e/D_{AB}	δ_{ave}
1	0.58	1.0	1.91	0.78	0.56	0.20	3.5	He	H_2	0.204	0.193	0.170	
								He	N_2	0.318	0.124	0.161	3.2
								O_2	N_2	1.12	0.035	0.192	
2a	0.66	1.9	2.54	0.75		0.23		He	H_2	0.430			
								He	N_2	0.675			
								O_2	N_2	2.70			
2b	0.68	1.6	1.91	0.75	0.51	0.23	2.4	He	H_2	0.275	0.125	0.110	
								He	N_2	0.420	0.082	0.115	4.3
								O_2	N_2	1.43	0.024	0.132	
2c	0.66	1.8	1.27	0.74		0.23		He	H_2	0.168			
								He	N_2	0.260			
								O_2	N_2	0.790			
3	0.83	3.0	1.91	0.70	0.38	0.28	0.9	He	H_2	0.560	0.066	0.058	
								He	N_2	0.883	0.042	0.059	6.4
								O_2	N_2	3.37	0.011	0.061	
4	1.02	5.5	1.91	0.66	0.28	0.35	0.7	He	H_2	1.12	0.033	0.029	
								He	N_2	1.79	0.020	0.028	9.5
								O_2	N_2	6.37	0.0056	0.031	

° from helium-pycnometer data
°° β_a = macro porosity; values from mercury porosimeter data
† β_i = microporosity = 0.342 ρ_B. The micropore volume (0.342 cu.cm./g.) was taken from the average of Otani's measurements (3).

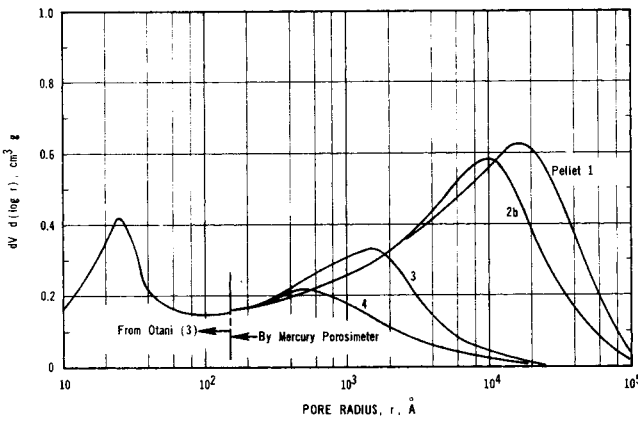

Fig. 3. Pore size distributions of alumina pellets.

helium pycnometer, and the bulk density ρ_B was determined from the weight and known volume of the mold. The macropore ($>$ 150 Å. radius)-volume distribution was measured for pellets 1, 2b, 3, and 4 using a mercury porosimeter. The micropore-volume distribution was taken from Otani (3) who obtained the distribution for the same Boehmite sample by nitrogen adsorption. The distribution curves are shown in Figure 3. The sum of the macro and micro porosities (Table 1) agree well with the total porosity determined independently from the pycnometer data. The average macropore radii shown in Table 1 are averages with respect to pore volume (*10*).

DIFFUSION RESULTS

As a first test of single pellet chromatography, response peaks were measured for three alumina pellets (2a, 2b, 2c) of different lengths but nearly the same density. Runs were made for three inert, tracer-carrier gas combinations for each pellet, as shown in Table 1. Experimentally, a pulse of tracer was injected for a small time τ, rather than an impulse input. Also, it was necessary to correct the measured first moment for the residence time V_{dead}/Q in the dead volume. Hence, Equation (19) becomes

$$\Delta\mu_1 = \frac{L^2}{D_e}\left(\frac{\beta}{2} + \frac{\gamma}{L}\right) \tag{21}$$

where

$$\Delta\mu_1 = (\mu_1)_{exp} - \frac{V_{dead}}{Q} - \frac{\tau}{2} \tag{22}$$

The values of $(\mu_1)_{exp}$ were calculated from $\mu_1 = m_1/m_0$, using the measured chromatographic peak to evaluate the integrals in Equation (16). Numerical integration (Simpson's rule) was used. The flow rate was maintained nearly the same for each run at about 30 cu.cm./min. (24°C., 1 atm.). Then $\Delta\mu_1$ was calculated from Equation (22).

According to Equation (21), $\Delta\mu_1/L^2$ plotted versus γ/L for the three pellets should give a straight line with an intercept on the abscissa (that is, for $\Delta\mu_1/L^2 = 0$) of $\gamma/L = -\beta/2$. Since $\beta = 0.75$ (from pycnometer measurement Table 1), this intercept establishes a common point on the lines for the three gas systems. Knowing that $\gamma = V_d/S = 0.70/[\pi/4\ (1.33)^2] = 0.50$ cm., values of γ/L are calculable for any pellet length. The data points do show a linear relationship, and a common intersection point, as indicated in Figure 4. The values for pellet 2c deviate slightly from the lines. This could be due to the slightly smaller void fraction for this pellet or due to difficulties in reproducing pore structures of different pellets, even though the pelletting pressure is the same.

The effective diffusivities were calculated from the slopes (equal to $1/D_e$) of these lines. The values for the three tracer-carrier systems are given in Table 1 in the row of data for pellet 2b. Since the results indicate that the equations predict the observed influence of pellet length, first moments for other pellet densities were measured for but one length (1.91 cm.). From such moments D_e was calculated directly from Equations (21) and (22), using known values of β. These results are also given in Table 1.

As the average radius of the macropores is large (Table 1), diffusion through these pellets is predominantly in the macropores and occurs by a bulk-diffusion mechanism. However, tracer gas moves in and out of the micropores as the pulse diffuses through the pellet. Since the diffusion path is very short in the small particles containing the micropores, transport resistance is negligible in the micropores. Then D_e in Equation (22) is the macropore diffusivity and is related to the tortuosity factor, for the parallel-pore model, by the expression

$$\frac{D_e}{D_{AB}} = \frac{\beta_a}{\delta} \tag{23}$$

For a single pellet, the ratio D_e/D_{AB} should be the same for any gas system. The experimentally determined ratios are plotted versus β_a in Figure 5 and do indicate reasonably constant values for the three gas combinations. Tortuosity factors calculated from Equation (23) are given in Table 1. The bulk diffusivities used are the experimentally determined values reported in (*4*), except for O_2-N_2, for which D_{AB} was taken from (*6*). The magnitude of δ (3.2 for the lowest density pellet) is about as expected (*7*), as is the increase in δ with decreasing β_a. When diffusion is entirely in the macropore region, the random pore model (*10*) gives

$$\frac{D_e}{D_{AB}} = \beta_a^2 \tag{24}$$

or $\delta = 1/\beta_a$. This relationship also suggests a rapid increase in δ with decreasing β_a. However, the absolute

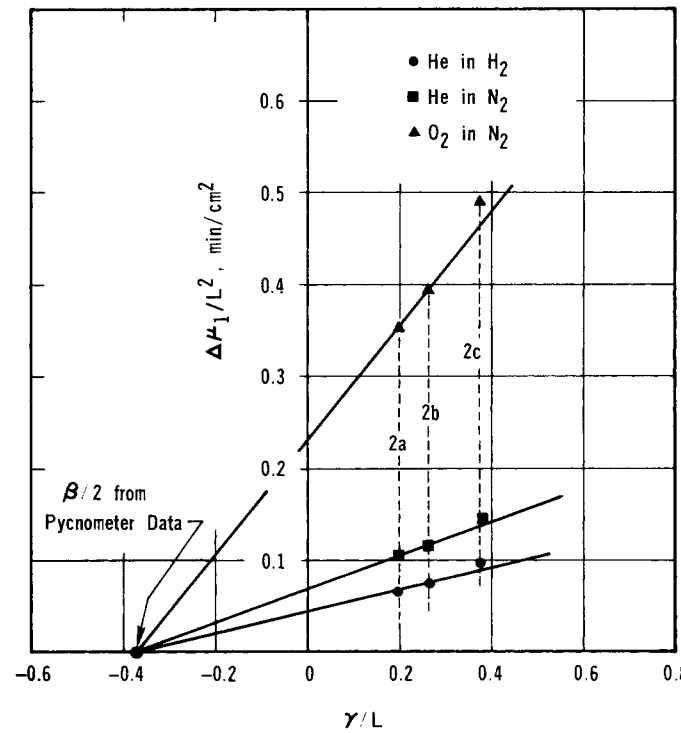

Fig. 4. $\Delta\mu_1/L^2$ versus γ/L for different pellet lengths (pellets 2a, b, c).

values of D_e/D_{AB} predicted by Equation (24) are considerably higher than the experimental results, as shown also in Figure 5. The proper porosity to use in Equation (21) is the total value β since it arises from the accumulation term in Equation (1). Nevertheless, if the diffusion is predominantly in the macropores, the tortuosity is correctly obtained by using the macropore porosity β_a in Equation (23).

The assumption of uniform concentration in the detector chamber can be tested by estimating the relaxation times according to the expressions given earlier. The relaxation time for the detector chamber is

$$\left(\frac{V_d}{S}\right)^2 \frac{1}{D_{AB}} = \frac{0.25}{D_{AB}}$$

For the inert systems ($K_a = 0$) employed with the alumina pellets the relaxation time for the pellets is, utilizing Equation (23),

$$L^2\beta/D_e = \frac{L^2\beta\ \delta}{D_{AB}\ \beta_a}$$

Pellet 2c provides the most severe test. Using the data in Table 1 for this pellet

$$\frac{L^2\beta}{D_e} \approx \frac{(1.27)^2(0.74)4.3}{0.51\ D_{AB}} = \frac{10}{D_{AB}}$$

The ratio of relaxation times of pellet to detector chamber is about 40 in the most conservative case. For pellet 4 this ratio is about 320 and for adsorbable gases it would be higher. Therefore, when V_d/S is small enough the assumption of uniform concentration in the detector chamber should not cause significant error.

ADSORPTION AND DIFFUSION FOR NICKEL CATALYST

As a test of the method for an adsorbable component system, response peaks were measured for the D_2(tracer) — H_2(carrier) system with a Nickel/Kieselguhr catalyst. This system had been studied previously (5, 9) using a long bed of catalyst particles. The earlier work demonstrated that the linear rate expression, Equation (5), may be employed for deuterium exchange, provided a pseudo rate constant k_a^* and pseudo equilibrium constant K_a^* replace k_a and K_a. These quantities are

$$k_a^* = \frac{R}{C_t} \qquad (25)$$

$$K_a^* = \frac{n_t}{C_t} \qquad (26)$$

where R is the exchange rate of hydrogen between gas and surface, and C_t and n_t are the corresponding total gas and adsorbed concentrations.

Experiments

For these experiments the catalyst holder (Figure 2b) was filled with unconsolidated particles. Complete reduction of the catalyst was more easily assured using such assemblies of particles than for pellets. The particles were prepared by crushing Nickel/Kieselguhr hydrogenation pellets [G-49B from Chemetron Corp., Catalysts Division] and retaining the 60 to 80 mesh size material (average radius 0.114 mm.). The particles were held in place on a stainless steel screen (see insert Figure 2b), and a gas disperser was attached to the feed nozzle to reduce the possibility of a pressure-induced flow through the particles.

The particle properties and the properties of the unconsolidated beds held in the mold are given in Table 2. The macropore porosity was calculated from the known particle density, the mass of particles in the mold, and its volume.

The first peaks were measured for the inert He(tracer) — N_2(carrier) system in order to establish the tortuosity factor in the unconsolidated particles. Data were obtained for both the active catalyst (used later for the D_2-H_2 runs) and for the original, stabilized form. For the inert system there was no observable effect of activation, probably because the original form from the manufacturer was already in a partially reduced state. The activation involved placing the entire cell in an oven at 300°C. and passing H_2 through the particles at a flow of 10 cu.cm./min. The tube carrying the hydrogen leaving the cell was immersed in a dry-ice bath. The flow was continued until no condensation of water was observed in the immersed tube. Afterwards the flow of hydrogen was increased to 30 cu.cm./min. for another 2 hr. The cell was then cooled and replaced in the system, taking care to maintain a hydrogen atmosphere in the cell.

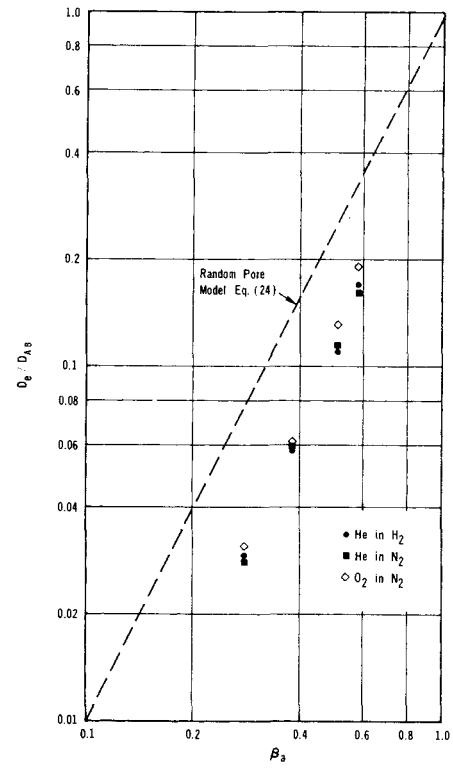

Fig. 5. D_e/D_{AB} versus macropore porosity, β_a.

TABLE 2. DATA FOR ASSEMBLIES OF NICKEL CATALYST PARTICLES

Bed no.	Length, cm.	β_{ep}	Catalyst condition	System tracer-carrier	$(\Delta\mu_1)_{ave}$,° min.
1	5.08	0.390	stabilized	He N_2	0.913
2	3.82	0.395	stabilized	He N_2	0.552
3	3.18	0.393	active	He N_2	0.429
				D_2 H_2	3.54
4	2.54	0.400	active	D_2 H_2	2.28
5	1.90	0.397	active	D_2 H_2	1.38

Properties of particles (5): $\beta_p = 0.58$, $\rho_p = 1.73$ g./cu.cm.

° Average of five measurements; ranges of scattering for $\Delta\mu_1$ are shown in Figure 6 by arrows.

As Table 2 indicates, chromatographic curves were measured for three lengths of particle assemblies for both inert and adsorbing systems. The base line of the peaks was less stable for the D_2-H_2 adsorption runs. Average values of $\Delta\mu_1$, obtained from Equation (22) are given in the table.

Diffusion Results

The first moments for the He-N_2 system are plotted in Figure 6 (lower part) for the three lengths. As for the alumina pellets, the intercept on the abscissa (equal to $-\beta/2$) was used to aid in locating the line. This value of β was essentially the same for all three lengths, since β_a was nearly the same, and is equal to the sum of the inter- and intra-particle porosities, 0.393 + 0.58 (1 − 0.393) = 0.74. The slope of the line so located, which is equal to $1/D_e$ (Equation (21), gives D_e = 12.5 sq.cm./min. For these assemblies of unconsolidated particles, diffusion is only significant in the interparticle space where the porosity is 0.393. Hence the tortuosity factor for the interparticle space is, using an expression analogous to Equation (23),

$$\delta = \frac{\beta_{ep} D_{AB}}{D_e} = \frac{0.393\ (42.6)}{12.5} = 1.35$$

where D_{AB} for He-N_2 was taken from (4). A value of 1.35 is reasonable for diffusion in an unconsolidated assembly of particles.

Next, this value for δ was employed to calculate D_e for the D_2-H_2 system. Taking D_{AB} = 75.0 sq.cm./min. (4),

$$(D_e)_{D_2\text{-}H_2} = \frac{\beta_{ep} D_{AB}}{\delta} = \frac{0.398\ (75.0)}{1.35} = 21.9 \text{ sq.cm./min.}$$

Adsorption Results

Knowing D_e, the first moment data for the reduced catalyst and the D_2-H_2 system can be used to establish K_a^* and the equilibrium adsorption. First, the data for assemblies 3, 4, and 5 are plotted (Figure 6, upper part) and a straight line located with a slope of $1/D_e$. This line is then compared with Equation (17). In terms of $\Delta\mu_1$, this equation becomes

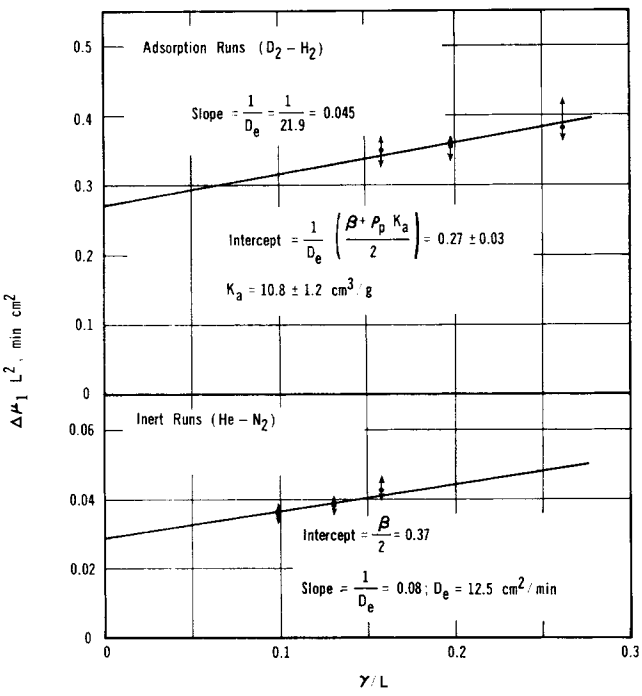

Fig. 6. $\Delta\mu_1/L^2$ plots for catalyst particle assemblies.

$$\frac{\Delta\mu_1}{L^2} = \frac{1}{D_e}\left(\frac{\beta + \rho_B K_a^*}{2} + \frac{\gamma}{L}\right) \qquad (27)$$

According to Equation (27) the value of $\Delta\mu_1/L^2$ at the intercept, where $\gamma/L = 0$, will be

$$\left(\frac{\Delta\mu_1}{L^2}\right)_{\gamma/L=0} = \frac{1}{D_e}\left(\frac{\beta + \rho_B K_a^*}{2}\right)$$

or

$$K_a^* = \frac{2D_e}{\rho_B}\left(\frac{\Delta\mu_1}{L^2}\right)_{\gamma/L=0} - \beta/\rho_B \qquad (28)$$

The intercept read from Figure 6 gives K_a^* = 10.8 ± 1.2 cu.cm./g. The uncertainty level is estimated from the maximum variation in locating the line in Figure 6 due to scatter of the data. The bulk density of the particles, necessary for application of Equation (28), is given by $\rho_p(1 - \beta_{ep})$ = 1.73 (1 − 0.398) = 1.04 g./cu.cm.

The adsorbed concentration n_t at equilibrium is, from Equation (26),

$$n_t = 10.8\,\frac{1.0}{82\ (297)} = 4.4 \times 10^{-4} \text{ moles/g.}$$

Measurements of K^* at other total pressures would establish the adsorption isotherm. Padberg's value (5) of n_t at 24°C. for the same catalyst was 4.6 × 10^{-4} moles/g.

The use of single pellet chromatography gave a consistent value of the equilibrium adsorption in this case. The result was improved by independent measurements of the tortuosity factor using data for the He-N_2 system. In principle it is possible to evaluate both D_e and K_a^* from data for the adsorbing system alone. Thus, measurement of $\Delta\mu_1$ for two different values of L, and simultaneous solution of the expressions obtained by applying Equation (27) to the two points, would be sufficient to establish D_e and K_a^*. However, the scatter in $\Delta\mu_1$, due to the somewhat unstable base line, and the small value of γ/L relative to that of $(\beta + \rho_p K_a^*)/2$ [see Equation (27)] prevented accurate results by this method.

SECOND MOMENTS

Second moments are more sensitive to tailing of chromatographic peaks and, therefore, are usually less accurate than first moments. Because of their sensitivity μ_2' values provide a severe test of the consistency of the measurements and validity of the model used to interpret the data. The only rate parameter involved in the expression [Equation (20)] for μ_2' for an inert gas is D_e. Hence, second moments provide no more rate information about the pellet than do first moments. However, the general reliability of D_e values obtained from $\Delta\mu_1$ for the alumina pellets can be evaluated with second-moment information. The D_e results in Table 1 were used in Equation (20) to calculate μ_2'. Before comparison, the experimental μ_2' should be corrected for the second moment of the input pulse ($\tau^2/12$, assuming a square pulse) and for the dispersion in V_d. Since these corrections were negligible in our work, the two μ_2' values can be compared directly with the results shown by the solid points in Figure 7. There seems to be no systematic deviation between $(\mu_2')_{exp}$ and $(\mu_2')_{calc}$. Note that the percentage difference in some instances is large and characteristic of the scatter observed in second moments. The open triangles show the same results for the inert data obtained with the unconsolidated assemblies of nickel catalyst particles.

The second moment for the adsorbable system, D_2-H_2, includes the effect of the adsorption rate constant k_a^*, as shown by the last term in Equation (18). Using the values of k_a^* and K^* obtained in reference 9, at 24°C. and 1 atm.,

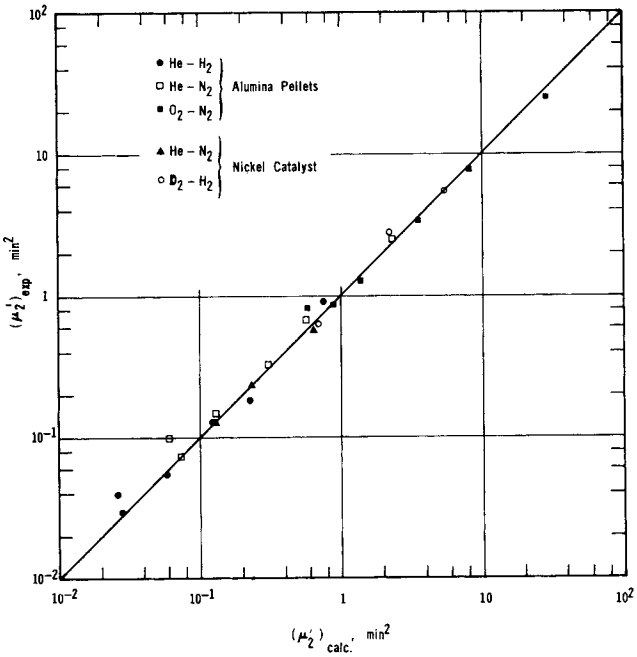

Fig. 7. Comparison of experimental and calculated [from Equations (18) or (20)] second moments.

this term is estimated to be about three orders of magnitude smaller than the other terms in Equation (18). Therefore, μ_2' calculated from the first two terms (which do not involve k_a^*), using D_e and K_a determined previously from the first moment data, should agree with $(\mu_2')_{exp}$. The open circles in Figure 7 verify this expectation. The small magnitude of the last term in Equation (18) also means that for the conditions of our experiments it is not possible to evaluate adsorption rate constants. Equation (18) shows that the last term increases with respect to the others for smaller L and k_a and larger D_e. It would appear difficult experimentally to obtain accurate μ_2' at much lower L and larger D_e than the values corresponding to our conditions. Hence determination of k_a by single pellet chromatography seems to be doubtful.

CONCLUSIONS

Single pellet chromatography offers another method for obtaining the effective diffusivity of gases in porous catalysts. It is rapid and requires no calibration of the concentration-measuring detector as long as linearity exists between the detector signal and the concentration. This is because only the moments of the chromatographic peak are used. First-moment information is sufficient, but second-moment results provide a sensitive test of the reliability of the experiments.

It is also possible to evaluate adsorption equilibrium data from first moments using an adsorbable tracer. With the isotope technique it is not necessary that adsorption rate be linear. In principle, measurements for pellets of different lengths are adequate to obtain both D_e and the adsorption equilibrium constant. However, for accurate results it may be advisable to evaluate the tortuosity factor of the pellet independently by obtaining first moments for a nonadsorbable system.

Our studies have not uncovered conditions suitable for evaluating adsorption rate constants by single pellet chromatography, although this is possible by chromatographic experiments in packed beds (5, 9).

ACKNOWLEDGMENT

The financial support of the National Science Foundation, Grant GK 2243, is gratefully acknowledged. Also, the Chemetron Corporation, Catalysts Division, kindly donated the nickel catalyst material.

NOTATION

C = concentration, g.-mole/cu.cm.; $\overline{C}$ = Laplace transform of $C(t)$
C_L = concentration at the detector
D_e = effective diffusivity, sq.cm./sec.
D_{AB} = molecular (bulk) diffusivity, sq.cm./sec.
K_a = adsorption equilibrium constant (K_a^* = pseudo value), cu.cm./g.
k_a = adsorption rate constant (k_a^* = pseudo value), cu.cm./g.-sec.
$k(p)$ = defined by Equation (12), g.-min./cu.cm.
L = length of pellet or assembly of particles, cm.
M = strength of impulse of tracer input, g.-mole
m_n = nth moment function of $C_L(t)$, min.$^{n+1}$-g.-mole/cu.cm.
n = adsorbed concentration on catalyst surface, g.-mole/g.; $\overline{n}$ = Laplace transform of $n(t)$
p = Laplace transform parameter, sec.$^{-1}$
Q = volumetric flow rate, cu.cm./min.
R = exchange rate between gas phase and catalyst surface, g.-mole/g.-sec.
r = radius of pore, Å.
S = cross sectional area of pellet, sq.cm.
t = time, sec. or min.
X = x/L
x = distance from end face of pellet in direction of diffusion, cm.
V_{dead} = volume between tracer injection and pellet face, cu.cm.
V_d = volume of detector chamber, cu.cm.

Greek Letters

β = total porosity of pellet or assembly of particles
β_a = porosity of macropores ($\overline{r} > 150$Å.)
β_{ep} = porosity in interparticle region of assembly of particles
β_i = porosity in micropores
β_p = void fraction of particle
γ = characteristic length of the detector = V_d/S, cm.
δ = tortuosity factor
$\delta(t)$ = delta function input
Λ = defined by Equation (11)
μ_1 = first absolute moment, min.
μ_2' = second central moment, min.^{2}
ρ_B = bulk density of pellet or assembly of particles, g./cu.cm.
ρ_p = particle density, g./cu.cm.
τ = injection time of pulse, min.

LITERATURE CITED

1. Balder, J. R., and E. E. Petersen, *J. Catalysis*, **11**, 195, 202 (1968).
2. Gibilaro, L. G., F. Gioia, and G. Greco Jr., *The Chem. Eng. Journal*, **1**, 85 (1970).
3. Otani, S., and J. M. Smith, *J. Catalysis*, **5**, 332 (1966).
4. Fuller, E. N., P. D. Schettler, and J. C. Giddings, *Ind. Eng. Chem.*, **58**, 19 (1966).
5. Padberg, G., and J. M. Smith, *J. Catalysis*, **12**, 172 (1968).
6. Perry, J. H., ed., "Chemical Engineer's Handbook," Fourth Edn., McGraw-Hill, New York (1963).
7. Satterfield, C. N., "Mass Transfer in Heterogeneous Catalysis," M.I.T. Press, Cambridge, Mass. (1970).
8. Schneider, P., and J. M. Smith, *AIChE J.*, **14**, 762, 886 (1967).
9. Suzuki, M., and J. M. Smith, *J. Catalysis*, **23**, 321 (1971).
10. Wakao, N., and J. M. Smith, *Chem. Eng. Sci.*, **17**, 825 (1962).

Manuscript received July 6, 1971; revision received September 22, 1971; paper accepted September 23, 1971.